JACS
JOURNAL OF THE AMERICAN CHEMICAL SOCIETY
Communication
pubs.acs.org/JACS

A Molecular Balloon: Expansion of a Molecular Gyrotop Cage Due to Rotation of the Phenylene Rotor

Wataru Setaka*,†,‡ and Kentaro Yamaguchi*,†

†Faculty of Pharmaceutical Sciences at Kagawa Campus, Tokushima Bunri University, 1314-1 Shido, Sanuki, Kagawa 769-2193, Japan
‡Precursory Research for Embryonic Science and Technology (PRESTO), Japan Science and Technology Agency (JST), 4-1-8 Honcho Kawaguchi, Saitama 332-0012, Japan

Supporting Information

ABSTRACT: A macrocage molecule with a bridged phenylene rotor has been reported as a molecular gyrotop, because the rotor can rotate even in a crystalline state. Although the most stable cage structure of the molecular gyrotop in a crystal was folded and shrunken at low temperature, expansion of the cage was observed at high temperature due to rapid rotation of the phenylene in a crystal. This phenomenon is analogous to the deflation and inflation of a balloon. Moreover, the unusually large thermal expansion coefficient of the crystal was estimated in the temperature range in which the expansion of the cage was observed, indicating a new function of dynamic states of the molecules.

Much attention is currently focused on the chemistry and other properties of molecular machines, in which the mechanical motions of parts of the molecules are observed.[1] While there are many well-known molecular-scale materials based on the static state, the application of molecular motion has the potential to yield a large number of novel functional materials. A macrocage molecule with a bridged rotor was first proposed as a molecular gyroscope by Garcia-Garibay and co-workers,[2] as the rotor can rotate even in a crystalline state. The chemistry of molecular gyroscopes, molecular gyrotops, and related molecules has been reported by Garcia-Garibay et al.,[3] Gladysz et al.,[4] our group,[5] and other researchers.[6] In addition, the kinetics of a related molecular gyroscope has been reported as temperature dependence of the dielectric loss.[7]

Recently, we reported thermal modulation of birefringence in a crystal of molecular gyrotop **1** that has a phenylene rotor encased in three long alkyl-spokes.[8] The result was the first application of an optical property change due to dynamic equilibrium states of the phenylene rotor in the crystal. In this report, we demonstrate a new function of the dynamic equilibrium state in a molecular gyrotop: an expansion of the cage due to rapid rotation of the rotor observed in a crystal of a novel molecular gyrotop **2**.

The molecular gyrotop **2** is a intermediate in the synthesis of the molecular gyrotop **1**.[8] Therefore, the molecular gyrotop **2** was synthesized by ring closing metathesis of *p*-bis(tri-7-octenylsilyl)benzene (**3**) (Scheme 1).[8−10] The desired cage-like *E,E,E*-isomer (**2**) was isolated from the reaction mixture, which also included polymeric byproduct. Although several structural isomers of **2** are possible products for this reaction, their formation could not be detected by GPC or reversed-phase HPLC analysis of the reaction mixture. In addition, hydrogenation reaction of **2** at 3 atm hydrogen pressure with Pd/C as a catalyst gave compound **1** in 95% yield.

Scheme 1. Synthesis of Molecular Gyrotops 1 and 2

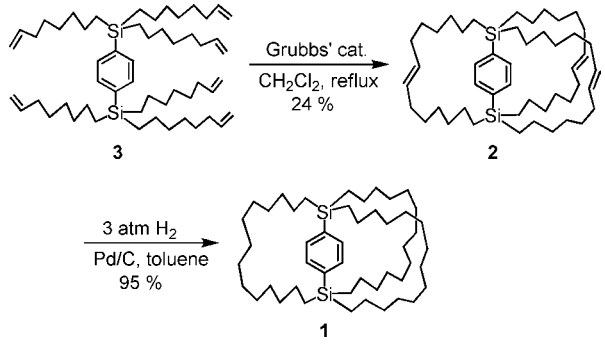

Figure 1a shows the molecular structure of **2** in the single crystal as determined by X-ray crystallography at 100 K.[11] Two of the three alkenyl chains were extended upward and downward against the bissilylbenzene moiety, causing the cage to appear dented and shrunken. This structural feature was different from that of **1**, where a spherical cage is evident.[8] The molecules were packed in crystals and arranged according to their rotation axes (Figure 1b).

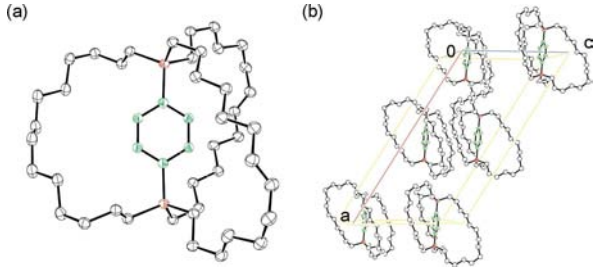

Figure 1. (a) Molecular structure of **2** in crystal form; 30% thermal probability ellipsoid. (b) Crystal packing diagram of **2**.

Solid-state ^{2}H NMR was employed to estimate the rate and angular range of the phenylene flip in the crystal.[8,12] Figure 2a shows temperature dependent quadrupolar echo ^{2}H NMR

Received: June 15, 2012
Published: July 16, 2012

   dx.doi.org/10.1021/ja305822e | J. Am. Chem. Soc. 2012, 134, 12458−12461

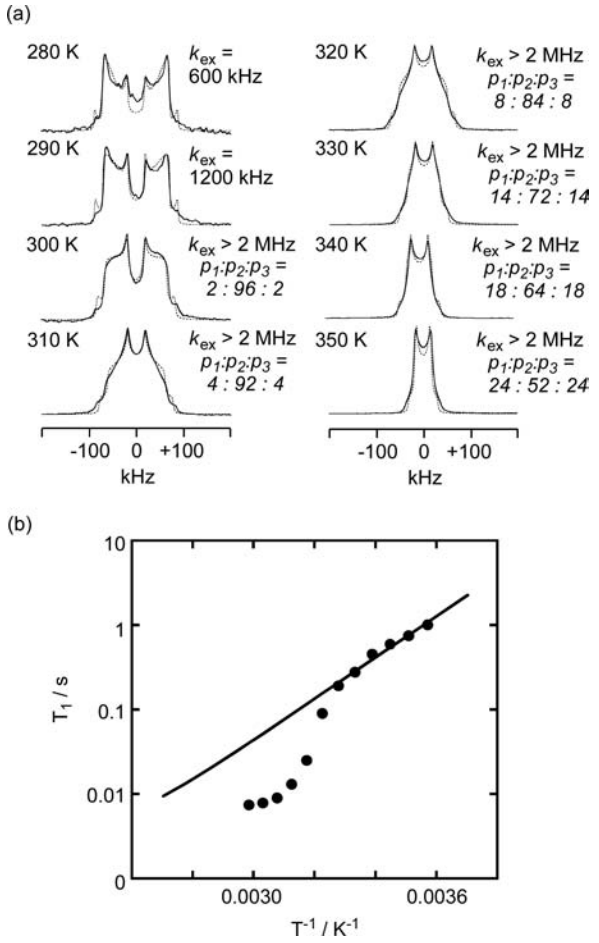

Figure 2. (a) Temperature dependence of solid-state ^{2}H NMR spectra of **2**-d_4 [Solid line: observed spectra; dotted line: simulated spectra. Below 290 K, a two-site exchange mechanism was applied, whereas above 300 K, a six-site exchange mechanism was applied assuming different populations. Designated exchange rate constants k and ratio of populations for each phenylene site (p_1:p_2:p_3) are shown.]. (b) Temperature dependence of the ^{2}H spin−lattice relaxation times (T_1) in molecular gyrotop **2** in crystal form. The lines are predicted based on the relaxation model (eq 1), whose parameters are listed as follows: $K = 5.8 \times 10^{10}$ Hz, $E_a = 11.2$ kcal/mol, $\omega_0/2\pi = 76.7$ MHz, $\tau_\infty = 1.00 \times 10^{-15}$ s.

spectra of **2**-d_4, in which the phenylene moiety was labeled with four deuterium atoms.[13] At 280 K the phenylene ring slowly undergoes a 180° flip between two equilibrium sites which were determined by X-ray structural analysis. The rates of flipping in the temperature range of 280−300 K were estimated by simulation of spectral line shapes (Pake pattern).[14] The energy barrier (E_a) for the phenylene flip in **2** was estimated to be 11.4 kcal/mol by Arrhenius plot (see Supporting Information). Compared to the energy barrier for the flip of **1** (10.3 kcal/mol),[8] the value of **2** is large (11.4 kcal/mol). The higher energy barrier of **2** is probably due to the dented cage constructed by rigid alkenyl-chains. Therefore the cage structure could affect the energy barrier for the phenylene flip in molecular gyrotops. Upon heating above 300 K, the line widths of the observed spectra became narrower and the shapes of the spectra were altered slightly. These spectral changes indicate continuous rotation of the phenylene in **2**-d_4 with an exchange frequency over the fast limit (>2 MHz). The observed spectra were simulated by assuming a six-site exchange mechanism and applying different populations of benzene rings that can exist at three positions every 120° around an axis of rotation. The simulated spectra accurately reproduced the observed spectra, as shown in Figure 2a. These results indicate that there are disorders in the phenylene positions above 310 K. This dynamic behavior in the temperature dependent ^{2}H NMR spectra is completely reversible in the temperature range of 280−350 K.

To confirm the mechanism of the phenylene dynamics of **2**-d_4, the temperature dependence of the spin−lattice relaxation time (T_1) of solid-state ^{2}H NMR spectroscopy was investigated.[8] The T_1 for the molecular gyrotops was measured using the inversion−recovery quadrupole echo pulse sequence.[13] The rate of relaxation was known to be fit to eq 1, when the reorientational motion can be described by an exponential correlation function and the temperature dependence of the correlation time follows Arrhenius behavior.[8,15]

$$\frac{1}{T_1} = K\left(\frac{\tau}{1+\omega_0{}^2\tau^2} + \frac{4\tau}{1+4\omega_0{}^2\tau^2}\right)$$
$$\text{where } \tau = \tau_\infty \, e^{E_a/RT} \qquad (1)$$

Here K is an effective coupling constant, $\omega_0/2\pi$ is the Larmor frequency of deuterium, and τ is a single correlation time. Figure 2b compares the experimental results of the ^{2}H NMR spin−lattice relaxation measurements of molecular gyrotop **2**-d_4 to the calculated spin−lattice relaxation times. According to the model for the rate of relaxation (eq 1), the observed T_1 agreed with the calculated T_1 in the temperature range of 240−310 K. The fitted parameters calculated by eq 1 are shown in the caption of Figure 2b. The activation energy of 11.2 kcal/mol is consistent with those derived from the analysis of the Pake pattern of the ^{2}H NMR spectra. On the other hand, above 310 K, the observed T_1 values were different from the calculated ones, indicating that different activation energies for the phenylene dynamics should be employed.

To elucidate the reason behind the change in the phenylene dynamics above 310 K, X-ray crystallographic studies were performed above this temperature. Figure 3b shows the molecular structure in a crystal at 340 K. As expected, a disordered benzene ring was observed at three positions around an axis of rotation. Moreover, a remarkable change in the shape of the cage was observed: the cage assumed a sphere-like structure, different from that observed at 100 K (Figure 1) and 300 K (Figure 3a). It is plausible that the cage assumed a

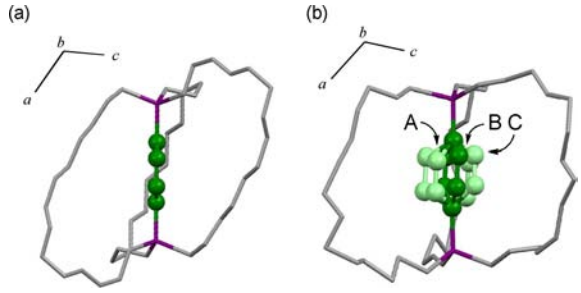

Figure 3. Temperature dependence of the molecular structure of **2** in crystal form determined by single crystal X-ray crystallography: (a) 300 K, (b) 340 K. The disordered phenylene ring is observed at three positions A, B, and C with occupancy factors of 0.239(15), 0.463(15), and 0.292(13), respectively. (Directions of unit-cell axes are shown.)

dx.doi.org/10.1021/ja305822e | J. Am. Chem. Soc. 2012, 134, 12458−12461

sphere-like shape in order to avoid steric contact between itself and the phenylene rotor rotating rapidly inside the cage at high temperatures. These structural changes caused the change in the energy barrier for the phenylene dynamics above 310 K, as described in the T_1 study in the ^{2}H NMR experiment.

The change in the cage structure, due to dynamics of the phenylene rotor, can also cause a remarkable deformation of the unit cell of the crystal. Powder synchrotron X-ray diffraction (XRD) studies of molecular gyrotop **2** were carried out to determine the temperature dependence of the crystal parameters of the unit cell.[16] The results are summarized in Figure 4a. Although the cell parameters were almost constant

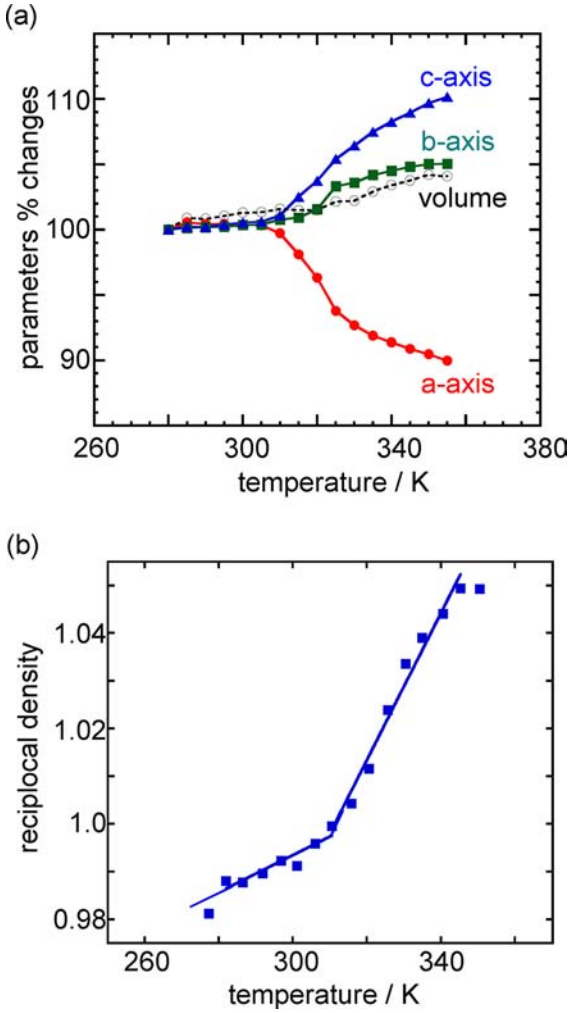

Figure 4. (a) Plots of the relative variations in the cell axes and volume vs temperature for compound **2**: (●) *a* axis, (■) *b* axis, (▲) *c* axis, and (○) volume. The values are normalized to the data at 277 K (100%). (b) Reciprocal plot of the density of the unit cell determined by powder XRD as a function of the temperature for compound **2**.

below 310 K, they were gradually altered above this temperature. Therefore, the structural change was discontinuous, with the phase transition at 310 K, and above this, it was altered continuously by acceleration of the dynamics of the phenylene rotor. In this high temperature region, the size of the *a*-axis became shorter and the *c*-axis became larger. Because the direction of the change is identical to the structural change of the cage (cf. Figure 3), the deformation of the unit cell is likely caused by the structural change of the cage as a result of rapid rotation of the phenylene rotor inside the crystal. When the powder sample was left at 355 K for a long time (over 5 min), an irreversible phase transition occurred. After the phase transition the cell parameters were different from the present data, unfortunately the parameters have not been specified.

As the variation in cage structure was due to expansion, remarkable volume expansion of the crystal should be observed. The reciprocal plot of the density of the unit cell determined by XRD as a function of the temperature is shown in Figure 4b. The data of molecular gyrotop **1**, whose cage structure only slightly expanded with increasing temperature, are shown in Figure S8 (Supporting Information). The slope of the plot corresponds to the volume expansion coefficient of the crystal. In the case of molecule **1**, the expansion coefficient in the temperature range of 220−360 K is estimated to be $466 \pm 17 \times 10^{-6}$ K^{-1} (see Supporting Information). This is the normal value for common organic crystals, such as benzene (350×10^{-6} K^{-1} [−183 to −79 °C]), naphthalene (280×10^{-6} K^{-1} [−20 to 70 °C]), and anthracene (190×10^{-6} K^{-1} [−195 to 22 °C]).[17] In the case of molecule **2**, the volume expansion coefficient of $389 \pm 67 \times 10^{-6}$ K^{-1} below 310 K is almost identical to that of molecule **1**. The unusually large expansion coefficient of **2** is estimated to be $1540 \pm 92 \times 10^{-6}$ K^{-1} in the temperature range of 310−350 K, indicating expansion of the cage inside the crystal. This expansion coefficient is comparable to thermal expansion coefficients in the liquid phase (for example, benzene 1229×10^{-6} K^{-1} [0 to 30 °C] or naphthalene 853×10^{-6} K^{-1} [82 to 115 °C][17]).

In summary, because the phenylene rotor occupied an equilibrium position for a sufficient time, the most stable cage structure of molecular gyrotop **2** was folded and shrunken at low temperatures. Expansion of the cage due to rapid rotation of the phenylene of the molecular gyrotop took place to prevent steric contact between the cage and rotor, and the molecule converted thermal energy into internal energy by the rotation of the phenylene rotor. As a result, the most stable cage structure of the molecule at high temperature was a expanded, sphere-like shape. This phenomenon is analogous to the deflation and inflation of a balloon. Therefore, molecular gyrotop **2** was classified as a functional molecular balloon.

■ ASSOCIATED CONTENT

Ⓢ Supporting Information

Details for solid-state ^{2}H NMR study of **2**, X-ray diffraction studies (single crystal and powder) of **2** and analysis of the thermodynamic expansion coefficient of **1** by XRD. This material is available free of charge via the Internet at http://pubs.acs.org.

■ AUTHOR INFORMATION

Corresponding Author

setaka@kph.bunri-u.ac.jp; yamaguchi@kph.bunri-u.ac.jp

Notes

The authors declare no competing financial interest.

■ ACKNOWLEDGMENTS

We thank Dr. K. Miura (BL19B2, BL38B1), Dr. K. Osaka (BL19B2), Dr. S. Baba (BL38B1), and Dr. N. Mizuno (BL38B1) for the support X-ray diffraction experiment in the Spring-8. This work was supported by a Grant-in-Aid for Scientific Research on Inovation Areas "Emergence in

Chemistry" (20111007) from the Japanese Ministry of Education, Culture, Sports, Science and Technology (MEXT).

REFERENCES

(1) (a) Vogelsberg, C. S.; Garcia-Garibay, M. A. *Chem. Soc. Rev.* **2012**, *41*, 1892−1910. (b) Karim, A. R.; Linden, A.; Baldridge, K. K.; Siegel, J. S. *Chem. Sci.* **2010**, *1*, 102−110. (c) Blanzani, V.; Credi, A.; Venturi, M. *Molecular Devices and Machines*, 2nd ed.; Wiley-VCH: Weinheim, 2008. (d) Leigh, D. A.; Zerbetto, F.; Kay, E. R. *Angew. Chem., Int. Ed.* **2007**, *46*, 72−191. (e) Browne, W. R.; Feringa, B. L. *Nat. Nanotechnol.* **2006**, *1*, 25−35. (f) Kelly, T. R. *Molecular Machines*; Topics in Current Chemistry, Vol. *262*; Springer: Hidelberg, 2005. (g) Kottas, G. S.; Clarke, L. I.; Horinek, D.; Michl, J. *Chem. Rev.* **2005**, *105*, 1281−1376. (h) Garcia-Garibay, M. A. *Proc. Natl. Acad. Sci. U.S.A.* **2005**, *102*, 10771−10776. (i) Blanzani, V.; Credi, A.; Raymo, R.; Stoddart, J. F. *Angew. Chem., Int. Ed.* **2000**, *39*, 3348−3391.

(2) (a) Dominguez, Z.; Dang, H.; Strouse, M. J.; Garcia-Garibay, M. A. *J. Am. Chem. Soc.* **2002**, *124*, 2398−2399. (b) Godinez, C. E.; Zepeda, G.; Garcia-Garibay, M. A. *J. Am. Chem. Soc.* **2002**, *124*, 4701−4707. (c) Dominguez, Z.; Dang, H.; Strouse, J. M.; Garcia-Garibay, M. A. *J. Am. Chem. Soc.* **2002**, *124*, 7719−7727. (d) Dominguez, Z.; Khuong, T. A. V.; Sanrame, C. N.; Dang, H.; Nuñez, J. E.; Garcia-Garibay, M. A. *J. Am. Chem. Soc.* **2003**, *125*, 8827−8837.

(3) (a) Commins, P.; Nuñez, J. E.; Garcia-Garibay, M. A. *J. Org. Chem.* **2011**, *76*, 8355−8363. (b) Nuñez, J. E.; Natarajan, A.; Khan, S. I.; Garcia-Garibay, M. A. *Org. Lett.* **2007**, *9*, 3559−3561.

(4) (a) Wang, L.; Hampel, F.; Gladysz, J. A. *Angew. Chem., Int. Ed.* **2006**, *45*, 4372−4375. (b) Narwara, A. J.; Shima, T.; Hampel, F.; Gladysz, J. A. *J. Am. Chem. Soc.* **2006**, *128*, 4962−4963. (c) Shima, T.; Hampel, F.; Gladysz, J. A. *Angew. Chem., Int. Ed.* **2004**, *43*, 5537−5540.

(5) (a) Setaka, W.; Ohmizu, S.; Kira, M. *Chem. Lett.* **2010**, *39*, 468−469. (b) Setaka, W.; Ohmizu, S.; Kabuto, C.; Kira, M. *Chem. Lett.* **2007**, *36*, 1076−1077.

(6) (a) Khan, N. S.; Perez-Aguilar, J. M.; Kaufmann, T.; Hill, P. A.; Taratula, O.; Lee, O.-S.; Carroll, P. J.; Saven, J. G.; Dmochowski, I. J. *J. Org. Chem.* **2011**, *76*, 1418−1424. (b) Kitagawa, H.; Kobori, Y.; Yamanaka, M.; Yoza, K.; Kobayashi, K. *Proc. Natl. Acad. Sci. U.S.A.* **2009**, *106*, 10444−10448. (c) Sugino, H; Kawai, H.; Fujiwara, K; Suzuki, T. *Chem. Lett.* **2012**, *41*, 79−81.

(7) (a) Horansky, R. D.; Clarke, L. I.; Winston, E. B.; Price, J. C.; Karlen, S. D.; Jarowski, P. D.; Santillan, R.; Garcia-Garibay, M. A. *Phys. Rev. B* **2006**, *74*, 054306. (b) Horansky, R. D.; Clarke, L. I.; Price, J. C.; Khuong, T.-A. V.; Jarowski, P. D.; Garcia-Garibay, M. A. *Phys. Rev. B* **2005**, *72*, 014302.

(8) Setaka, W.; Yamaguchi, K. *Proc. Natl. Acad. Sci. U.S.A.* **2012**, *109*, 9271−9275.

(9) (a) Phan, S. T.; Setaka, W.; Kira, M. *Chem. Lett.* **2007**, *36*, 1180−1181. (b) Phan, S. T.; Setaka, W.; Kira, M. *Chem. Lett.* **2008**, *37*, 976−977.

(10) Synthesis of the Molecular Gyrotop **2**: To a solution of dichloromethane (500 mL) in the presence of Grubbs' catalyst, first generation (0.05 g, 0.06 mmol), a dichloromethane solution (200 mL) of *p*-bis(tri-7-octenyl)silylbenzene[8] (**3**, 1.42 g, 1.78 mmol) was added dropwise with stirring over 12 h, and the mixture was further stirred for 12 h. The volatile materials were removed in vacuo, and the benzene soluble fraction was treated with flash column chromatography (silica gel, benzene). By GPC (chloroform), fractions containing **2** were collected. Pure compound **2** (310 mg, 0.43 mmol, 24% yield) was obtained by recrystallization from tetrahydrofuran/methanol (4:1). **2**: colorless crystals, mp 202−203 °C; ^{1}H NMR ($CDCl_3$, 400 MHz): δ 0.71−0.76 (m, 12H, Si−CH_2−), 1.20−1.35 (m, 48H), 1.90−2.00 (m, 12H, −HC═CH−CH_2−), 5.32 (t, J = 3.6 Hz, 6H, alkenyl -HC═C*H*−), 7.46 (s, 4H, aromatic C*H*); ^{13}C NMR ($CDCl_3$, 100 MHz): δ 13.29, 23.64, 27.85, 28.85, 32.27, 33.07, 130.47 (alkenyl *C*H), 133.64 (aromatic *C*H), 137.15 (Si*C*); ^{29}Si NMR ($CDCl_3$, 79.5 MHz): δ −2.14; UV−vis (hexane solution): λ_{max}/nm(ε) 231 (15,100), 270 (590), 265 (580); Anal. Calcd for $C_{48}H_{82}Si_2$: C, 80.59; H, 11.55. Found: C, 80.60; H, 11.72.

(11) X-ray crystallographic analysis of **2** was carried out at the BL38B1 beamline in SPring-8 with the approval of the Japan Synchrotron Radiation Research Institute (JASRI) (Proposal No. 2009B1035). Crystal data of **2** (100 K, λ = 0.7000 Å): monoclinic, *C*2/*c*, *a* = 29.831(1) Å, *b* = 10.971(1) Å, *c* = 16.524(1) Å, β = 123.193(1)°, *V* = 4525.4 Å^3, R_1 = 0.0674 ($I > 2\sigma I$), wR_2 = 0.1909 (all data). Crystallographic data were deposited in the Cambridge Crystallographic Database Centre (CCDC-780905). Details for the X-ray structural analyses of **2** at 300 and 340 K were shown in SI.

(12) Cholli, A. L.; Dumais, J. J.; Engel, A. K.; Jelinski, L. W. *Macromolecules* **1984**, *17*, 2399−2404.

(13) Temperature-dependent solid-state ^{2}H NMR spectra were recorded on Varian Unity 500 spectrometers, using a quadrupolar echo pulse sequence (d1−90° pulse-τ_1-90° pulse-τ_2-FID; 90° pulse = 4.2 μs, τ_1 = 30 μs, τ_2 = 20 μs, d1 = 20 s). Simulations of ^{2}H NMR spectra were carried out on *NMR-WEBLAB*.[14] The following parameters were used for simulation: quadrupolar coupling constant q_{cc} = 140 kHz, asymmetry parameter η = 0, line broadening = 3 kHz. Details are given in the SI. Temperature dependences of the spin−lattice relaxation time (T_1) in ^{2}H NMR spectra were recorded using an inversion−recovery quadrupolar echo pulse sequence (d_1−180° pulse-d_2−90° pulse-τ_1-90° pulse-τ_2-FID; 90° pulse = 4.2 μs, τ_1 = 30 μs, τ_2 = 20 μs, d_1 = 5−3 s, d_2 were varied) and standard T_1 analysis software.

(14) Macho, V.; Brombacher, L.; Spiess, H. W. *Appl. Magn. Reson.* **2001**, *20*, 405−432.

(15) The spin lattice relaxation rate is known to depend on the motional model for the exchange process. Several special types of the motions have been discussed so far, see: Spiess, H. W. *NMR Basic Principles and Progress*; Diehl, P., Fluck, E., Kosfeld, R., Eds.; Springer: Heidelberg, 1978. Further detailed investigations are required in order to determine parameters for the appropriate special model.

(16) Powder X-ray diffraction (XRD) was carried out at the BL19B2 beamline in SPring-8 with the approval of the JASRI using a diffractometer equipped with a Debye−Scherrer IP camera (Proposal No. 2010A1771). Details are given in the SI.

(17) Schäfer, K., Beggerow, G. *Landolt-Börnstein Zahlenwerte und Funktionen aus Physik Chemie, Astronomie, Geophysik und Technik, 6 Aufl., II Band, 1 Teil*; Eucken, A., Ed.; Springer-Verlag: Berlin, 1971; pp 436−714.